Available online at www.scholarsresearchlibrary.com

Scholars research library

Archives of Applied Science Research, 2011, 3 (5):506-513
(http://scholarsresearchlibrary.com/archive.html)

ISSN 0975-508X
CODEN (USA) AASRC9

Preparation and electrical properties of nanocrystalline $MgFe_2O_4$ oxide by combustion route

Sachin V. Bangale*, D.R.Patil and S. R. Bamane

Metal Oxide Research, Laboratory, Department of Chemistry, Dr. Patangrao Kadam Mahavidyalaya, Sangli (M.S.) India

---

ABSTRACT

Semiconductive nanoparticles of $MgFe_2O_4$ were synthesized by a solution combustion technique. The process was a convenient, environment friendly, inexpensive and efficient method for synthesis of $MgFe_2O_4$ nanoparticles. The synthesized materials were characterized by TG/DTA, XRD, and TEM. Electrical properties of the synthesized nanoparticles are studied by AC conductivity measurement. Electrical conductivity of the nanomaterial $MgFe_2O_4$ was increased with the temperature.

Keyword: Nanostructure $MgFe_2O_4$, XRD, SEM, TEM, Gas sensor.

INTRODUCTION

Spinal of the type M^{2+} $M_2^{3+}O_4$ attract the research interest because of their versatile practical application [1-2]. Spinel ferrites with the general formula AFe_2O_4 (A = Mn, Co, Ni, Mg, or Zn) are very important magnetic materials because of their interesting magnetic and electrical properties with chemical and thermal stabilities [3]. Magnesium ferrite ($MgFe_2O_4$) is one of the most important ferrites. It has a cubic structure of normal spinel-type and is a soft magnetic n-type semiconducting material, which finds a number of applications in heterogeneous catalysis, adsorption, sensors, and in magnetic technologies [4-5]. Recently, nanostructures of magnetic materials have received more and more attention due to their novel material properties that are significantly different from those of their bulk counterparts [6-9]. Current years have been increased interests in study the gas sensing properties of ferrites [10-12]. Gopal reddy et al. reported the response of copper ferrite ($CuFe_2O_4$) and zinc ferrite ($ZnFe_2O_4$) for hydrogen sulfide (H_2S) and that of nickel ferrite ($NiFe_2O_4$) for chlorine gas (Cl_2) [10]. One of the present authors (Y-L.Liu) also confirmed that $ZnFe_2O_4$ possessed gas sensing properties for H_2S

[11].magnesium ferrite ($MgFe_2O_4$) is one of the important ferrites with spinel structure [13]. It is used as a catalyst [14] and humidity sensor [15]. It is also an n-type semiconductor with the band gap of 2.18V [16].

The need for a novel gas sensor capable of providing reliable operation in harsh environment is now greater than ever. Such sensors find a range of application, including the monitoring of traffic pollutants or food quality with specially designed electronic noses [17-18]. Gas sensors based on metal oxides are commonly used in the monitoring of toxic pollutants and can provide the necessary sensitivity, selectivity and stability required by such system [19]. Commonly used oxides include zinc oxide, titanium dioxide, iron oxide, tungsten oxide and tin oxide. These materials have successfully been employed to detect a range of gas vapours, particularly ethanol, methanol and propanol [20-21].

Among various materials used for sensing application, ferrite is used as a good class of sensing materials. But they suffer a drawback of being at higher temperature [22]. Consequently, it is interesting to investigate the gas-sensing properties of $MgFe_2O_4$. The gas sensing efficiency of the materials depends on its microstructural properties which are related to its method of preparation, the later plays a very important role with regard to the chemical, structural and properties of a spinel ferrite. $MgFe_2O_4$ is routinely synthesized by combustion method of precursors zinc nitrate, magnesium nitrate and glycine as fuel [23]. Alternatively, a number of wet method including coprecipitation [24], sol-gel [25], microemulsions [26], oxidation techniques [27] and hydrothermal synthesis [28]. An ideal process should be environmentally friendly and should be as simple as possible. A novel preparation technique of nanomaterial, combustion synthesis at ambient conditions, has been developed to prepared nanosized compounds. It was a high-yielding, low-cost and facile synthesis method.

In this paper, we have synthesized $MgFe_2O_4$ nanoparticles by novel combustion reaction. One of our aims is to develop a general synthesis method and explore the gas sensing properties of the $MgFe_2O_4$ nanopowder. We found that the process is a convenient, environment friendly, inexpensive and efficient. Furthermore, the $MgFe_2O_4$ obtained possesses excellent gas-sensing responses to reducing gas and grain size is about 15-35 nm. Here the presented a static gas sensor using these nanoparticles. This discovery could aid in the synthesis of low cost and room temperature ammonia gas sensors.

MATERIALS AND METHODS

2.1 Powder preparation

In this study polycrystalline $MgFe_2O_4$ powder was prepared using combustion technique. The materials used as precursors were magnesium nitrate hexahydrate Mg $(NO_3)_2.6H_2O$, iron nitrate hexahydrate $Fe(NO_3)_26H_2O$and glycine (all these were purchased from AR Grade of Qualigen fine Ltd.India). All of them were of high purity (99.9%, 98%, and 99.9% respectively). Glycine possesses a high heat of combustion. It is an organic fuel providing a platform for redox reactions during the course of combustion. Initially the magnesium nitrate iron nitrate and are taken in the proportion 1:1:4 respectively and two moles of glycine were dissolved in a beaker slowly stirring by using glass rod clear solution was obtained. Then they formed solution was evaporated on hot plate in the temperature range of 70^0C to 80^0C resulting into a gives thick gel.

The gel was kept on a hot plate for auto combustion and heated in the temperature range of 170^0C to 180^0C.The nanocrystalline $MgFe_2O_4$ powder was formed within a few minutes and it was sintered at about 500^0C, 600^0C, 700^0C, and 800^0C for about 4h we when got a brown colour shining powder of nanocrystalline $MgFe_2O_4$[29-30].

2.2 Thick Film Preparation

The thixotropic paste was screen printed on a glass substrate in desired patterns. The films prepared were fired at 500^0C for 4 h. Silver contact were made by vacuum evaporation for electrical measurements.

2.3 Characterization Techniques

The as –prepared samples were characterized by TG/DTA thermal analyzer (SDT Q600 V 20.9 Build 20), XRD Philips Analytic X-ray B.V. (PW-3710 Based Model diffraction analysis using Cu-K_α radiation), A JEOL JEM–200 CX transmission electron microscope operating at 200 kV analysis.

RESULT AND DISCUSSION

3.1 Spinel structure and formation analysis

$$2C_2NH_3O_2 + (9/2)\ O_2 \rightarrow N_2\uparrow + 4CO_2\uparrow + 5H_2O\uparrow \quad (1)$$

$$Zn(NO_3)_3 + Fe(NO_3)_3 + 4C_2H_5NO_2 \rightarrow ZnFe_2O_4 + 8CO_2\uparrow + 10H_2O\uparrow + 5N_2\uparrow \quad (2)$$

The TG curve in Fig. 1 shows a minor weight loss step (20%) from 30 up to about 270^0C and two major weight loss steps from 270 to 455^0C (60%). No further weight loss was observed up to 1000^0C. The minor weight loss was related to the loss of moisture and trapped solvent (water and carbon dioxide) in the as-spun $MgFe_2O_4$ nanopowder, whereas the major weight loss was due to the combustion of organic matrix. On the DTA curve, main exothermic peaks were observed at ~290 and ~ 450^0C, suggesting the thermal events related to the decomposition of Mg and Fe nitrates along with the degradation by dehydration on the nanopowder, which was confirmed by a dramatic weight loss in TG curve at the corresponding temperature range (270–455^0C). The plateau formed between 455 and 1000^0C on the TG curve indicated the formation of crystalline $MgFe_2O_4$ as the decomposition product. As confirmed by XRD and FT-IR analyses as showed in Figs. 2 and 5 respectively.

3.2 XRD study

The XRD patterns of the calcined $MgFe_2O_4$ are shown in Fig. 2. All of the main peaks are indexed as the spinel $MgFe_2O_4$ in the standard data (JCPD No: 88-1935). The average crystallite sizes of $MgFe_2O_4$ samples were calculated from X-ray line broadening of the reflections of (220), (311), (400), (511), and (440) using Scherrer's equation (i.e., $D = 0.89k/(\beta \cos\theta)$, where k is the wavelength of the X-ray radiation, K is a constant taken as 0.89, h the diffraction angle, and b is the full width at half-maximum [31] , and were found to be 16 ± 4, 18 ± 1, 25 ± 2, and 26 ± 3 nm for the samples of $MgFe_2O_4$ calcined at 500, 600, 700, and 800^0C, respectively.

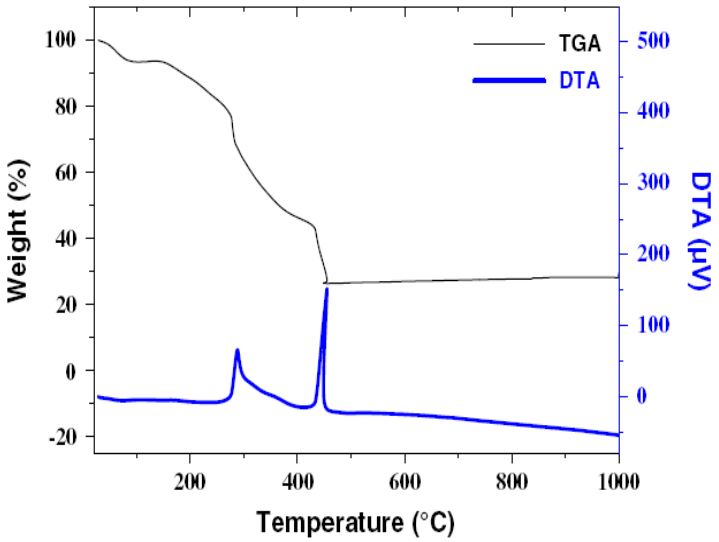

Fig. 1. TG-DTA curve of mixed precursor $MgFe_2O_4$.

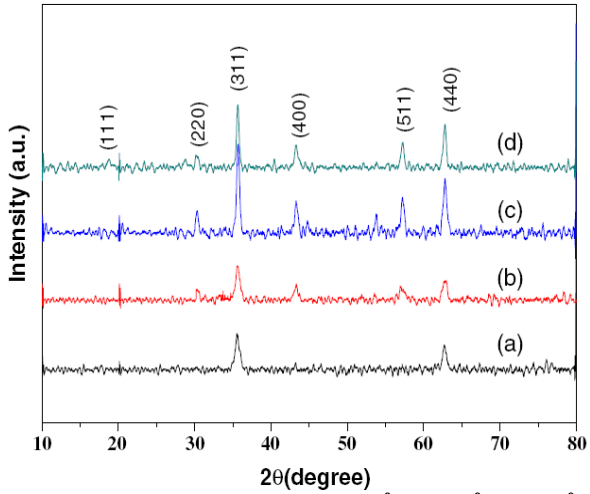

Fig.2 XRD pattern of calcinied mixed precursor $MgFe_2O_4$ at a 500^0C, b 600^0C, c 700^0C and d 800^0C in air for 4 h.

3.3 Particle size distribution studies.

Fig. 3 has been carried out by using dynamic light scattering techniques. (DLS *via* Laser input energy of 632 nm) It was observed that magnesium iron oxide nanoparticles have narrow size distribute within the range of about 10-15 nm. Which are well match with calculated value and was calculated it from Debye-Scherrer equation.

3.4 TEM studied

The detailed morphology and crystalline structure of the $MgFe_2O_4$ calcined at 700 and 800^0C for 4 h were further investigated by TEM, and the TEM bright-field images with corresponding selected-area electron diffraction (SAED) patterns of these two samples are shown in Fig.4. It is clearly seen from the TEM bright field images that both samples consisted of packed $MgFe_2O_4$ particles or crystallites with particle sizes of ~10–20 and 25–80 nm in diameter for the samples of 700^0C-calcined and 800^0C-calcined, respectively. It is seen that the particle sizes of $MgFe_2O_4$ contained in the calcined $MgFe_2O_4$ are quite uniform. Since the electro spun powder were very

standard data (JCPDS: 88-1935). The diffraction rings are identified as the (111), (220), (311), (400), (422), (511), and (440) planes. This concurs with the results of XRD presented in Fig. 2.

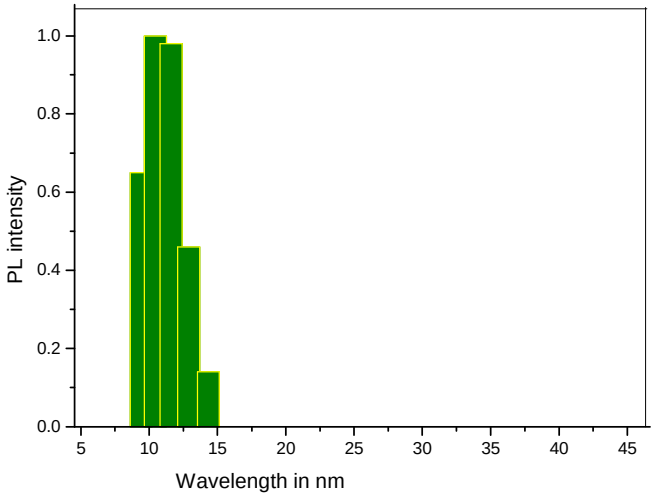

Fig.3 Particle size distribution studies

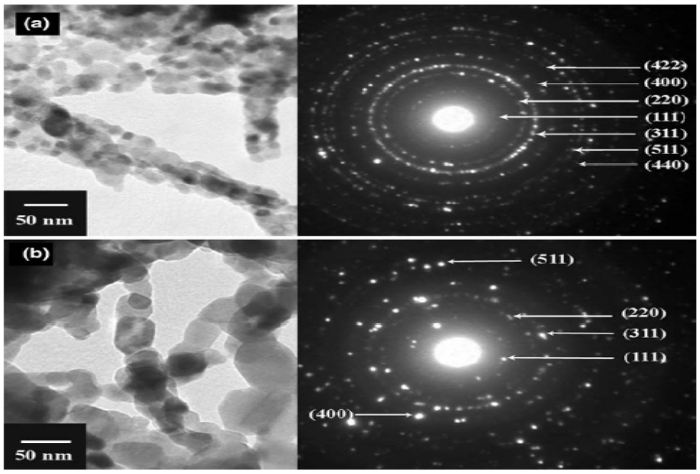

Fig.4 TEM images with corresponding SAED patterns of the $MgFe_2O_4$ samples calcined in air for 4 h at a 700^0C and b 800^0C.

3.5 FT-IR Studied

The formation of spinel $MgFe_2O_4$ structure in the calcined $MgFe_2O_4$ was further supported by FT-IR spectra (Fig.5). Here, we consider two ranges of the absorption bands: 4000–1000 and 1000–400 cm^{-1} as suggested by previously published studies [31-32]. In the range of 4000–1000 cm^{-1}, vibrations of CO_3^{2-} and moisture were observed. The intensive band at~~1627 cm^{-1} is due to O–H stretching vibration interacting through H bonds. The band at ~ 2920 cm^{-1} is C–H asymmetric stretching vibration mode due to the $–CH_2–$ groups of the long aliphatic alkyl groups. The υ(C=O) stretching vibration of the carboxylate group (CO_2^{2-}) was observed around 1380 cm^{-1} and the band at ~1016 cm^{-1} was corresponded to nitrate ion traces. Therefore the CO_3^{2-} and CO_3^{-} vibrations disappeared when calcinations temperature was increased. In the range

of 1000– 400cm^{-1}, a typical metal–oxygen absorption band for the spinel structure of the ferrite at ~560 cm^{-1} was observed in the FT-IR spectra of all of the calcined $MgFe_2O_4$ samples. This band strongly suggests the intrinsic stretching vibrations of the metal (Fe ↔ O) at the tetrahedral site [33].

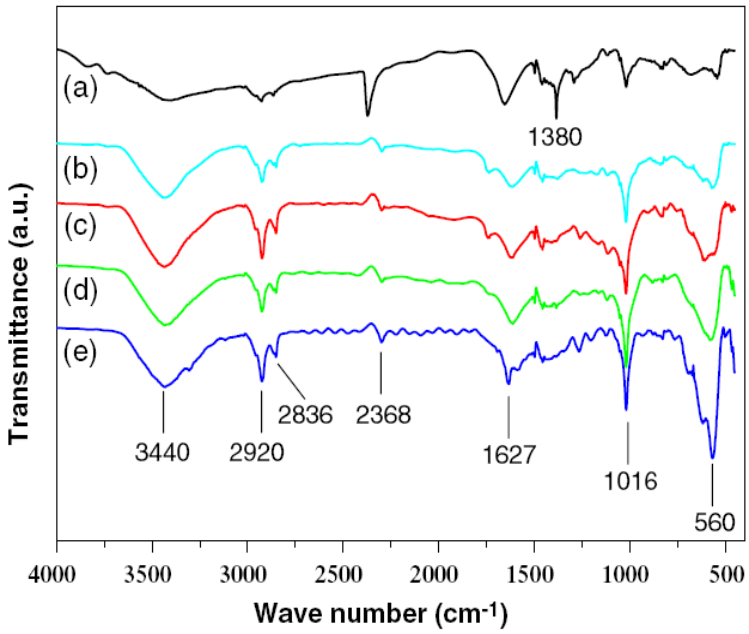

Fig. 5 FT-IR spectra of the $MgFe_2O_4$ composite samples calcined in air for 4 h at different temperatures. a As-spun, b 500^{0}C, c 600^{0}C, d 700^{0}C, and e 800^0 C.

4. Electrical properties

4.1 I-V characteristics

Fig.6 depicts I-V characteristics of $MgFe_2O_4$ films. It is clear from the symmetrical I-V characteristics that the silver contacts on the films were ohmic in nature.

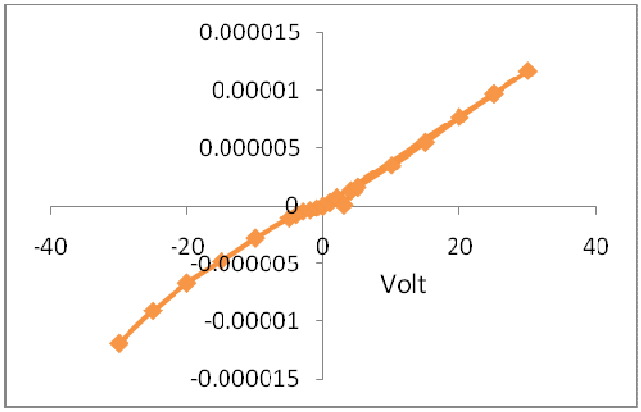

Fig.6 *I-V* characteristics of the sensor

4.2 Electrical conductivity

Fig.7 shows the variation of log (conductivity) with temperature. The conductivity values of sample increase with operating temperature. The increase in conductivity with increasing temperature could be attributed to negative temperature coefficient of resistance and semiconducting nature of $MgFe_2O_4$. It is observed from fig. 7 that the electrical conductivities of the $MgFe_2O_4$ films are nearly linear in the temperature range from 50- 400^0C in air ambient.

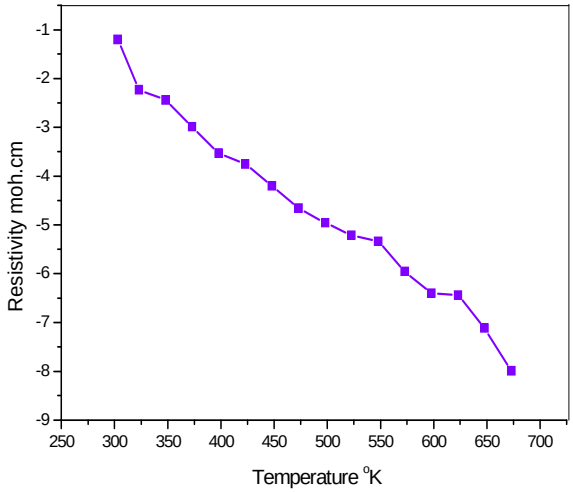

Fig.7. Variation of Resistivity with reciprocal operating temperature (K^{-1})

CONCLUSION

(I) Nanocrystalline $MgFe_2O_4$ has been synthesized by self combustion route. This synthesis route may be used for the synthesis of other metal oxide.
(II) These nanoparticles with show good I-V characteristics with ideal semiconducting nature at room temperature.
(III) Elemental analysis confirmed by using EDX. SEM micrographs show the material is porous in nature. TEM image shows grain size of the material was 16-26 nm.

REFERENCES

[1] Sugimoto M., *J.Am.Ceram.Soc.* ,**(1999)**, *82*, 269.
[2] Liu Y., Liu Z.M., Yang Y., Yang H.F., Shen G.L., Yu R.Q., *Sensors ans Actuators B* **(2005)**,*107*, 600-604.
[3] Hankare P.P., Jadhav S.D., Sankpal U.B., Patil R.P., Sasikala R., Mulla I.S., *Alloys and Compounds* ,**(2009)**, *488*, 270-272.
[4] Willey R.J., Noirclerc P., Busca G., *Chem.Eng.Commun*.,**(1993)**, 123.
[5] Oliver S.A.,Willey R.J.,Hamdeh H.H., Oliveri G., Busca G., *Scr.Mater*.,1995, *33*, **(1695)**.
[6] Wu W., He Q., Jiang C., *Nanoscale Res. Lett*., **(2008)**, *3*, 397.
[7] Hua Z.H., Chen R.S., Li C.L., Yang S.G., Lu M., Gu X.B., Du Y.W. *J. Alloys Compd*., **(2007)**, *427*, 199.
[8] Corr S.A., Rakovich Y.P., Gun'ko Y.K., *Nanoscale Res. Lett*.,**(2008)**, *3*, 87.

[9] Lai Z., Xu G., Zheng Y., *Nanoscale Res. Lett*., **(2007)**,*2*, 40.
[10] Gopal Reddy C.V.,.Manorama S.V, Rao V.J., *J.Mater. Sci.Lett*., **(2000)**, *19*, 775.
[11] Xinshu N., Yanli L., X.Jiaqiang, *Chin.Funct.Mater*., **(2002)**, *33*, 413.
[12] Satyanarayana L., Madhusudan K.,Reddy,V.M.Sunkara, *Mater.Chem.Phys*.,**(2003)**, *82*, 21.
[13] Liu C., Zou B., Rondinone A.J., Zhang Z.J. *J.Am.Chem.Soc*. , **(2000)**, *122*, 6263. [1
[14] Busca G., Finocchio E., Lorenzelli V., Trombetta M., Rossini S.A., *J.Chem.Soc. Faraday Trans*., **(1996)**, *92*, 4687.
[15] Shimizu Y., Arai H., T.Seiyama, *Sens.Actuators* ,**(1985)**, *7*, 11.
[16] Benko F.A., Koffyberg F.P., *Mater.Res.Bull*. **(1986)**, *21*, 1183.
[17] Sugimoto M., *J.Am.Ceram.Soc*. ,**(1999)**, *82*, 269-280.
[18] Kamble R.B.,.Mathe V.L, *Sensors and Actuatora B* , **(2008)**, *131*, 205-209.
[19] McMichael R.D., Shull R.D., L.J.Swartzendruber, Bennett L.H., Watson R.E., *J. Magn. Magn. Mater*.,**(1992)**, *11*, 29-33.
[20] Gopal Reddy C.V., Manorama S.V., Rao V.J., *J.Mater.Sci.Lett*. , **(2000)** , *9*, 775-778.
[21] Chen N.S., Yang X.J., Liu E.S., Huang J.L., *Sens. Actuators B* , **(2000)**, *66*, 178180.
[22] Rezlescu E., Popa P.D., N.Rezlescu , **(2006)**, *8*, 1016.
[23] Khetre S.M., Jadhav H.V., Jagdale P.N., Bangale S.V., Bamane S.R., *Advances in Applied Science Research*, **(2011)**, *2, (2)* , 252-259.
[24] Kodama T., Wada Y., Yamamoto T., Tsuji M., *J. Mater.Chem*. , **(1995)** , *5*, 1413.
[25] Hirano S., Yogo T., Kikuta K., Asai E., K.Sugiyama, Yamamoto H., *J.Am. Ceram. Soc*., **(1993)** ,*76*, 1788.
[26] Hochepied J.F., Bonville P., Pileni M.P., *J.Phys.Chem. B* , **(2000)** , *104*,905.
[27] Kiyama M., Bull., *Soc.Jpn*, **(1978)** , *51*, 134.
[28] Verma S., Joy P.A., Khollam Y.B., Potdar H.S., Deshpande S.B., *Mater.Lett*. **(2004)**, *58*, 1092.
[29] Bangale S. V., Khetre S. M. and Bamane S. R. , *Advances in Applied Science Research*, **(2011)**,*2*, 252-259.
[30] Sachin V. Bangale and Sambhaji R. Bamane Archives of Applied Science Research Vol. 3 No. 4, **(2011)**, 300-308
[31] Cullity B.D., Stock S.R., Elements of X-ray Diffraction (Prentice Hall, NJ, **(2001)**